PCP
PLANT & CELL PHYSIOLOGY

Functional Analysis of *Arabidopsis* CYP714A1 and CYP714A2 Reveals That They are Distinct Gibberellin Modification Enzymes

Takahito Nomura[1,3,6], Hiroshi Magome[1,4,6,*], Atsushi Hanada[1,5], Noriko Takeda-Kamiya[1,4], Lewis N. Mander[2], Yuji Kamiya[1,4] and Shinjiro Yamaguchi[1,5,*]

[1]RIKEN Plant Science Center, Tsurumi, Yokohama, Kanagawa 230-0045, Japan
[2]Research School of Chemistry, Australian National University, Canberra, ACT 0200, Australia
[3]Present Address: Weed Science Center, Utsunomiya University, Tochigi, 321-8505 Japan
[4]Present Address: RIKEN Center for Sustainable Resource Science, Tsurumi, Yokohama, Kanagawa 230-0045 Japan
[5]Present Address: Department of Biomolecular Sciences, Graduate School of Life Sciences, Tohoku, University, Sendai, Miyagi 980-8577, Japan.
[6]These authors contributed equally to this work.
*Corresponding authors: H. Magome, E-mail, hiroshi.magome@riken.jp; Fax +81-45-503-9662;
S. Yamaguchi, E-mail, shinjiro@m.tohoku.ac.jp; Fax +81-22-217-6197.
(Received June 4, 2013; Accepted August 27, 2013)

Endogenous levels of bioactive gibberellins (GAs) are controlled by both biosynthetic and inactivation processes, and some cytochrome P450s are involved in this control mechanism. We have previously reported that *CYP714B1* and *CYP714B2* encode the enzyme GA 13-oxidase, which is required for GA_1 biosynthesis, and that *CYP714D1* encodes GA 16α,17-epoxidase, which inactivates the non-13-hydroxy GAs in rice. *Arabidopsis* has two CYP714 members, *CYP714A1* and *CYP714A2*. To clarify the possible role of these genes in GA metabolism, enzymatic activities of their recombinant proteins were analyzed using a yeast expression system. We found that the recombinant CYP714A1 protein catalyzes the conversion of GA_{12} to 16-carboxylated GA_{12} (16-carboxy-16β,17-dihydro GA_{12}), a previously unidentified GA metabolite. Bioassays of this GA product showed that CYP714A1 is an inactivation enzyme in *Arabidopsis*. This was confirmed by the extreme GA-deficient dwarf phenotype shown by *CYP714A1*-overexpressing plants. Intriguingly, the recombinant CYP714A2 protein catalyzed the conversion of *ent*-kaurenoic acid into steviol (*ent*-13-hydroxy kaurenoic acid). When GA_{12} was used as a substrate for CYP714A2, 12α-hydroxy GA_{12} (GA_{111}) was produced as a major product and 13-hydroxy GA_{12} (GA_{53}) as a minor product. Transgenic *Arabidopsis* plants overexpressing the *CYP714A2* gene showed semi-dwarfism. GA analysis showed that the levels of non-13-hydroxy GAs, including GA_4, were decreased, whereas those of 13-hydroxy GAs, including GA_1 (which is less active than GA_4), were increased in the transgenic plants. Our results suggest that the CYP714 family proteins contribute to the production of diverse GA compounds through various oxidations of C and D rings in both monocots and eudicots.

Keywords: *Arabidopsis* • Biosynthesis • cytochrome P450 • Gibberellin • Inactivation.

Abbreviations: 16-carboxy GA_{12}, 16-carboxy-16β,17-dihydro GA_{12}; 2ODD, 2-oxoglutarate-dependent dioxygenase; CaMV, Cauliflower mosaic virus; CPS, *ent*-copalyl diphosphate synthase; *eui*, *elongated uppermost internode*; GA13ox, GA 13-oxidase; GA2ox, GA 2-oxidase; GA20ox, GA 20-oxidase; GA3ox, GA 3-oxidase; GAMT, GA methyltransferase; GC-MS, gas chromatography–mass spectrometry; GID1, GIBBERELLIN INSENSITIVE1; KAO, *ent*-kaurenoic acid oxidase; KO, *ent*-kaurene oxidase; MS, Murashige–Skoog; PAC, paclobutrazol; RNAi, RNA interference; RT-PCR, reverse transcription PCR; SEM, standard error of the mean; WT, wild type.

Introduction

Gibberellins (GAs) are a class of diterpenoid hormones that promote growth in various stages of plant lifecycle: seed germination, stem elongation, leaf expansion and flowering. GAs are biosynthesized from geranylgeranyl diphosphate (C_{20}) via a multistep process (**Fig. 1**; reviewed by Yamaguchi 2008). More than 130 GA compounds have been identified, but only a few, such as GA_1 GA_3, GA_4 and GA_7, are known to be the bioactive forms. *Arabidopsis* mutants defective in GA biosynthesis show dwarfism, dark-green leaves and late flowering phenotypes (Fleet and Sun 2005). In *Arabidopsis*, GA_4, a non-13-hydroxylated bioactive GA, is predominant in vegetative tissue, and is synthesized through the non-13-hydroxylation pathway (**Fig. 1**). GA_1, a 13-hydroxylated bioactive GA, is synthesized from the early GA 13-hydroxylation pathway. The

Plant Cell Physiol. 54(11): 1837–1851 (2013) doi:10.1093/pcp/pct125, available online at www.pcp.oxfordjournals.org

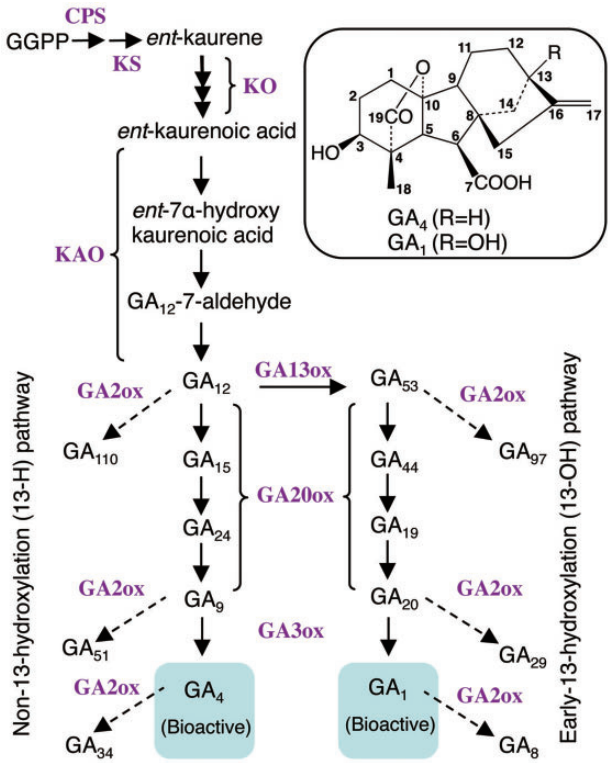

Fig. 1 GA biosynthesis and inactivation pathways in *Arabidopsis*. Solid and dashed lines indicate GA biosynthesis and inactivation (2β hydroxylation) pathways, respectively. GGDP, geranylgeranyl diphosphate; CPS, *ent*-copalyl diphosphate synthase; KS, *ent*-kaurene synthase; KO, *ent*-kaurene oxidase; KAO, *ent*-kaurenoic acid oxidase; GA20ox, GA 20-oxidase; GA3ox, GA 3-oxidase; GA2ox, GA 2-oxidase; GA13ox; GA 13-oxidase.

concentration of GA_1 is very low in vegetative tissues, but is higher in developing siliques (Varbanova et al. 2007, Kanno et al. 2010). GA_1 is less active than GA_4 both in *Arabidopsis* (Talon et al. 1990, Yang et al. 1995, Cowling et al. 1998) and in rice (Ueguchi-Tanaka et al. 2007), and this difference is presumably attributable to the binding affinity of these hormones to the GA receptor, GIBBERELLIN INSENSITIVE1 (GID1) (Ueguchi-Tanaka et al. 2005, Nakajima et al. 2006).

Recent studies revealed that multiple GA inactivation pathways are important for controlling endogenous GA levels in flowering plants (Yamaguchi 2008). Conjugation of glucose, resulting in the formation of glucose ethers or glucose esters, has been found in a number of plant species. This might be an inactivation reaction, but no GA-glycosyl transferase gene has been identified yet (Schneider and Schliemann 1994). So far, three classes of GA inactivation enzyme genes have been identified; 2-oxoglutarate-dependent dioxygenase (2ODD), methyltransferase and cytochrome P450 monooxygenase. GA 2-oxidase (GA2ox), which encodes 2ODD, converts bioactive and intermediate forms of GAs to inactive forms by 2β-hydroxylation (**Fig. 1**; Schomburg et al. 2003, Thomas et al. 1999). Thus far, seven *GA2ox* (candidate) genes (*GA2ox1-4* and *-6-8*; *GA2ox5* is a pseudogene) have been reported in *Arabidopsis* (reviewed by Yamaguchi 2008). Given the presence of orthologous *GA2ox* genes in a number of plant species, such as rice (Sakamoto et al. 2001), pea (Lester et al. 1999, Martin et al. 1999) and poplar (Busov et al. 2003), this inactivation is most common in flowering plants. The GA methyltransferase genes (*GAMT1* and *GAMT2*) have been identified in *Arabidopsis* (Varbanova et al. 2007). These genes are mainly expressed in developing and germinating seeds. The *gamt1* and *gamt2* double mutant exhibits elevated levels of bioactive GAs in siliques and shows resistance to a GA biosynthesis inhibitor, ancymidol, during germination. The rice cytochrome P450 monooxygenase CYP714D1 (EUI), represents a novel class of GA inactivation enzyme, which catalyzes 16α,17-epoxidation of non-13-hydroxy GAs (GA_{12}, GA_9 and GA_4) (Zhu et al. 2006). The *EUI* gene was identified by map-based cloning of the recessive rice mutant, *elongated uppermost internode* (*eui*). The mutant plants are morphologically normal until the drastic final internode elongation at the heading stage. Our GA analysis showed that exceptionally large amounts of the bioactive GAs GA_4 and GA_1 are accumulated in the uppermost internode of the *eui* mutant (Zhu et al. 2006). In contrast, overexpression of the P450 gene resulted in severe dwarfism in rice due to GA deficiency (Luo et al. 2006, Zhu et al. 2006).

Recently we reported that other rice CYP714 members, *CYP714B1* and *CYP714B2*, encode GA 13-oxidase (GA13ox), a key enzyme of the early GA 13-hydroxylation pathway (**Fig. 1**; Magome et al. 2013). The *cyp714b1 cyp714b2* double mutants showed decreased levels of 13-hydroxy GAs, including GA_1, but increased levels of non-13-hydroxy GAs, including GA_4. Like *eui* plants, the double mutant plants had elongated uppermost internodes at the heading stage. Our findings on the function of rice CYP714 members suggest that CYP714 proteins may also be involved in GA metabolism in other plant species. *Arabidopsis* has two CYP714 members, *CYP714A1* and *CYP714A2*, and it has been reported earlier that *CYP714A1*- or *CYP714A2*-overexpressing *Arabidopsis* plants show a severe dwarf phenotype (Zhang et al. 2011). Moreover, *CYP714A1* and *CYP714A2* double knockdown plants show increased aboveground biomass and early flowering with an increased level of bioactive GA_4. Based on these results, a possible functional overlapping of the CYP714A1 and CYP714A2 proteins in GA inactivation was proposed (Zhang et al. 2011). However, their enzymatic functions have not yet been identified. In this study, we investigated the possible role of these proteins in GA metabolism using a heterologous yeast expression system. We found that *CYP714A1* encodes a GA deactivation enzyme, which catalyzes 16-carboxylation of GA_{12}. Intriguingly, we found that CYP714A2 acts as a 13-oxidase or 12α-oxidase of GAs or GA precursors, depending on the substrate. GA analysis of *Arabidopsis* plants that overexpress *CYP714A2* showed that CYP714A2 could contribute to GA 13-hydroxylation in planta, indicating a functional kinship with rice CYP714Bs. Possible roles of CYP714A1 and CYP714A2 in GA metabolism are discussed.

Results

Functional analysis of the CYP714A1 and CYP714A2 proteins in a yeast expression system

We have previously shown that *CYP714D1/EUI* encodes the enzyme GA 16α,17-epoxidase, which inactivates the non-13-hydroxy GAs in rice (Zhu et al. 2006). More recently, we have reported that *CYP714B1* and *CYP714B2* genes encode GA13ox in rice (Magome et al. 2013). In *Arabidopsis* the CYP714A1 and CYP714A2 proteins share 73.1% identity in their amino acid sequences, and both are distantly related to rice CYP714Bs and CYP714D1 proteins (38.5–47.6%)(**Supplementary Table S1**). To clarify the possible function of these cytochrome P450s in GA metabolism, enzymatic activities of recombinant CYP714A1 and CYP714A2 proteins were analyzed using a yeast expression system. We first analyzed the enzymatic activity by incubating a microsomal fraction of *CYP714A1*- or *CYP714A2*-expressing yeast with various GAs as putative substrates, as we did for CYP714D1 (Zhu et al. 2006), but only small amounts of putative products were obtained in all cases. Such a reduced or loss of activity of plant P450s in the yeast microsomal fraction has been reported previously (Helliwell et al. 1999, Nomura et al. 2005). We therefore added various GAs (GA_{12}, GA_9, GA_4, GA_{53}, GA_{20} and GA_1) to a liquid culture of *CYP714A1*- or *CYP714A2*-expressing yeast cells, and the products were analyzed by full-scan gas chromatography–mass spectrometry (GC-MS).

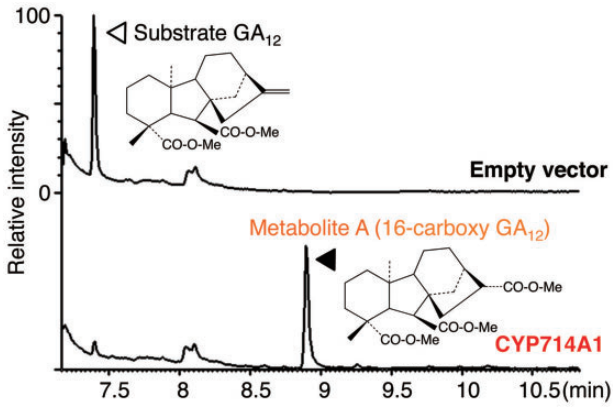

Fig. 2 Recombinant CYP714A1 protein has GA_{12} 16-carboxylation activity. Shown are total ion chromatograms (mass-to-charge ratio 50 to 600) of GA_{12} (upper, methyl ester derivative, indicated by an open triangle) and metabolite A (lower, methyl ester derivative, indicated by a closed triangle) after incubation of GA_{12} with control (empty vector) or CYP714A1-producing yeast culture. Metabolite A was identified as 16-carboxy GA_{12} (16-carboxy-16β,17-dihydro GA_{12}, **4**) by the retention time on GC and the mass spectrum listed in **Table 1**.

Recombinant CYP714A1 protein catalyzes 16-carboxylation of GA_{12}

Among the GA compounds mentioned above, GA_{12} (**1**) (bold numbers in parentheses refer to compounds indicated in **Supplementary Fig. S1**) was clearly metabolized by the *CYP714A1*-expressing yeast cells. A large fraction of the added GA_{12} was metabolized to a predominant product (designated metabolite A), whereas no conversion occurred when the control yeast carrying the empty vector was used (**Fig. 2**). Metabolite A was subsequently identified to be a 16-carboxylated GA_{12} (16-carboxy-16β,17-dihydro GA_{12}, designated in this paper as 16-carboxy GA_{12}, **4**) based on its retention time on GC and comparison of its mass spectrum with that of an authentic sample (**Table 1**). Meanwhile, we also found three other minor metabolites (B, C and D) (**Table 1**). Metabolite B

Table 1 GC-MS profiles of GA_{12} metabolites by recombinant CYP714A1 protein

Metabolite and reference sample	Retention time on GC (KRI)[a]	Characteristic ions, *m/z* (relative intensity)[b]
GA_{12} metabolite A[c]	2641	406 [M^+] (3), 374 (100), 359 (16), 342 (15), 314 (46), 287 (60), 259 (56), 227 (84), 199 (93)
Authentic 16-carboxy-16β,17-dihydro GA_{12}[c]	2640	406 [M^+] (3), 374 (100), 359 (16), 342 (15), 314 (47), 287 (61), 259 (55), 227 (85), 199 (93)
Authentic 16-carboxy-16α,17- dihydro GA_{12}[c]	2677	406 [M^+] (4), 374 (100), 359 (19), 342 (9), 314 (40), 287 (69), 259 (60), 227 (74), 199 (91)
GA_{12} metabolite B[d]	2798	523 [M^+-15] (1), 435 (100), 375 (27), 315 (4), 285 (5), 239 (6), 225 (7), 147 (28), 73 (75)
Authentic 16,17-dihydroxy-16α,17-dihydroGA_{12}[d]	2796	523 [M^+-15] (2), 435 (100), 375 (29), 315 (4), 285 (6), 239 (9), 225 (9), 147 (28), 73 (80)
GA_{12} metabolite C[d]	2658	450 [M^+] (1), 435 (24), 418 (42), 403 (9), 328 (37), 300 (100), 287 (18), 259 (28), 241 (95), 73 (100)
GA_{12} metabolite D[d]	2736	464 [M^+] (28), 449 (64), 432 (22), 389 (85), 357 (14), 329 (31), 301 (26), 223 (61), 73 (100)

[a]Kovats retention index.
[b]*m/z*, mass-to-charge ratio (M^+, molecular ion).
[c]Methyl ester derivative.
[d]Methyl ester-trimethylsilyl ether derivative.

was determined to be 16,17-dihydroxy-16α,17-dihydro GA_{12} (**5**), which was likely converted from 16α,17-epoxy GA_{12} in the presence of acetic acid during purification, as previously reported (Zhu et al., 2006). Metabolite C appeared to be 17-hydroxy-16ξ,17-dihydro GA_{12} (**6**) (Gaskin and Macmillan 1991), whereas metabolite D was unknown. GC-MS analysis of other GA compounds added as substrates showed no conversion, with the exception of GA_9 (**2**), which was converted to a putative oxidized product (16ξ,17-dihydroxy-16,17-dihydro GA_9, **3**) and two unknown products (data not shown).

When we used [17,17-$^2H_2$] GA_{12} as a substrate for CYP714A1, the product, 16-carboxy GA_{12} (**4**) carried a deuterium after derivatization to methyl esters, although there is no deuterium (hydrogen) at C17 (data not shown). Previous studies have shown that aldehydes RCH_2CHO are formed in addition to epoxides upon oxidation of the olefins $RCH=CH_2$ by rat liver microsomes in the presence of NADPH and O_2 (Mansuy et al. 1984). These aldehydes were not derived from the rearrangement of the epoxide, but are formed by the migration of a hydrogen within an intermediate with the active oxygen–iron complex. [16-^{2}H] 16β,17-dihydro-17-oxo GA_{12} might be produced from [17,17-$^2H_2$] GA_{12} by a similar mechanism, which might then have been further oxidized to form [16-^{2}H] 16-carboxy GA_{12}. We have used this labeled product as an internal standard to quantify endogenous ones in plants (see below).

Recombinant CYP714A2 protein has *ent*-kaurenoic acid 13-hydroxylation and GA_{12} 12α-hydroxylation activity

Next we examined the enzymatic activity of CYP714A2. Among the various GAs described above, only GA_{12} (**1**) was converted by the *CYP714A2*-expressing yeast culture; a large fraction of the added substrate was metabolized to a predominant product (metabolite E) (**Fig. 3A**). This metabolite was identified as 12α-hydroxy GA_{12} (GA_{111}, **13**) by comparison of the retention time on GC and the mass spectrum with that of an authentic sample (**Table 2**, **Supplementary Fig. S1**). We also found two minor products (F and G) (**Fig. 3A**, **Table 2**). Intriguingly, product F was identified as 13-hydroxy GA_{12} (GA_{53}, **14**), while product G was identified as 12α,13-dihydroxy GA_{12} (GA_{123}, **16**) by comparison with respective authentic samples on GC-MS. The ratio of these GA_{12} products was 100 (12α-hydroxy, **13**): 6 (13-hydroxy, **14**): 6 (12α,13-dihydroxy, **16**), calculated based on the relative intensity on the total ion chromatogram. The conversion of GA_{12} (**1**) to GA_{53} (**14**) by 13-hydroxylation is believed to be a key step of the early GA 13-hydroxylation pathway (**Fig. 1**) (Magome et al. 2013). But as shown above, 13-hydroxylation activity of the recombinant CYP714A2 protein was low when GA_{12} (**1**) was used as a substrate. This result implies the presence of other substrates more preferential than GA_{12} (**1**) for the 13-hydroxylation activity. Therefore, we tested three upstream precursors (*ent*-kaurenoic acid, **7**; *ent*-7α-hydroxy kaurenoic acid, **8**; and GA_{12}-7-aldehyde, **9**) of GA_{12} (**1**) for this assay. When *ent*-kaurenoic acid was

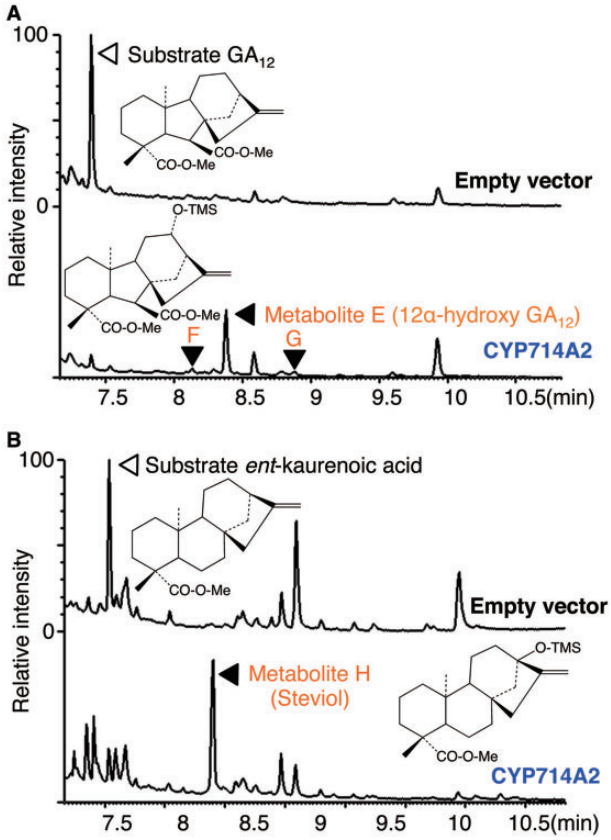

Fig. 3 Recombinant CYP714A2 protein has GA_{12} 12α-hydroxylation and *ent*-kaurenoic acid 13-hydroxylation activity. (A) Shown are total ion chromatograms (mass-to-charge ratio 50 to 600) of GA_{12} (upper, methyl ester derivative, shown by an open triangle) and metabolites E, F and G (lower, methyl ester-trimethylsilyl ether derivative, each shown by a closed triangle) after incubation of GA_{12} with control (empty vector) or CYP714A2-producing yeast culture. Metabolites E, F and G were identified as 12α-hydroxy GA_{12} (GA_{111}, **13**), 13-hydroxy GA_{12} (GA_{53}, **14**) and 12α,13-dihydroxy GA_{12} (GA_{123}, **16**), respectively by their retention times on GC and the mass spectra listed in **Table 2**. (B) Shown are total ion chromatograms of *ent*-kaurenoic acid (upper, methyl ester derivative, shown by an open triangle) and metabolite H (lower, methyl ester-trimethylsilyl ether derivative, shown by a closed triangle) after incubation of *ent*-kaurenoic acid with control (empty vector) or CYP714A2-producing yeast culture. The metabolite H was identified as steviol (*ent*-13-hydroxy kaurenoic acid, **10**) (**Table 2**).

added as a substrate, steviol (*ent*-13-hydroxy kaurenoic acid, **10**) was detected as the sole product (metabolite H) (**Fig. 3B**, **Table 2**). In addition, another metabolite, which is probably *ent*-7α,13-dihydroxy kaurenoic acid (**11**) (Gaskin and Macmillan 1991), was detected as the sole product of *ent*-7α-hydroxy kaurenoic acid metabolism (**8**) (**Supplementary Table S2**). When GA_{12}-7-aldehyde (**9**) was added as a substrate, a large amount of 12ξ-hydroxylated (**15**) and a small amount of 13-hydroxylated (**12**) derivatives (Gaskin and Macmillan 1991) were detected as probable metabolites (**Supplementary Table S2**, **Supplementary Fig. S1**), as was the case with the

Table 2 GC-MS profiles of GA_{12} and *ent*-kaurenoic acid metabolites by recombinant CYP714A2 protein

Metabolite and reference sample	Retention time on GC (KRI)[a]	Characteristic ions, *m/z* (relative intensity)[b]
GA_{12} metabolite E[c]	2560	448 [M^+] (2), 416 (24), 388 (16), 298 (34), 239 (55), 209 (65), 207 (76), 181 (45), 180 (47), 73 (100)
Authentic 12α-hydroxy GA_{12}[c]	2560	448 [M^+] (2), 416 (29), 388 (19), 298 (45), 239 (65), 209 (69), 207 (78), 181 (50), 180 (49), 73 (100)
Authentic 12β-hydroxy GA_{12}[c]	2580	448 [M^+] (3), 416 (30), 388 (20), 298 (42), 239 (51), 209 (68), 207 (78), 181 (46), 180 (46), 73 (100)
GA_{12} metabolite F[c]	2517	448 [M^+] (26), 416 (6), 389 (10), 251 (17), 235 (16), 208 (81), 207 (100), 193 (24), 181 (60), 73 (64)
Authentic GA_{53}[c]	2518	448 [M^+] (21), 416 (6), 389 (8), 251 (17), 235 (16), 208 (78), 207 (100), 193 (24), 181 (62), 73 (72)
GA_{12} metabolite G[c]	2643	536 [M^+] (23), 504 (7), 477 (9), 433 (25), 420 (14), 251 (17), 193 (62), 181 (55), 147 (30), 73 (100)
Authentic 12α,13-dihydroxy GA_{12}[c]	2643	536 [M^+] (22), 504 (7), 477 (10), 433 (24), 420 (14), 251 (16), 193 (65), 181 (56), 147 (31), 73 (100)
ent-Kaurenoic acid metabolite H[c]	2473	404 [M^+] (9), 389 (3), 348 (3), 214 (8), 193 (100), 180 (7), 73 (58)
Authentic steviol (*ent*-13-hydroxy kaurenoic acid)[c]	2473	404 [M^+] (9), 389 (3), 348 (3), 214 (8), 193 (100), 180 (6), 73 (48)

[a]Kovats retention index.
[b]*m/z*, mass-to-charge ratio (M^+, molecular ion).
[c]Methyl ester-trimethylsilyl ether derivative.

GA_{12} substrate. These results suggest that CYP714A2 is a bifunctional enzyme that preferentially catalyzes the C-13 hydroxylation of the *ent*-kaurane carbon skeleton (*ent*-kaurenoic acid, **7**; *ent*-7α-hydroxy kaurenoic acid, **8**) and the C-12 hydroxylation of the *ent*-gibberellane carbon skeleton (GA_{12}-7-aldehyde, **9**; GA_{12}, **1**).

Biological activity of CYP714A1 and CYP714A2 products

To clarify the role of CYP714As in *Arabidopsis*, we examined the biological activity of the products of these enzymes using the *Arabidopsis ga1-3* mutant (**Table 3**). The *ga1-3* mutant has a null mutation in the *ent-copalyl diphosphate synthase* (*CPS*) gene in an early step of the GA biosynthesis pathway, resulting in the inability of the seeds to germinate without exogenous treatment with GA (Sun and Kamiya 1994). Due to their commercial unavailability, we used 16-carboxy GA_{12} (**4**) and 12α-hydroxy GA_{12} (**13**) prepared enzymatically in this assay (see Materials and Methods). We found that the bioactive GA_4 was the most effective (100% germination with 1 μM GA_4) in inducing *ga1-3* seed germination, and GA_1, a 13-hydroxylated bioactive GA, was effective to a lesser extent (32% germination with 1 μM GA_1). Treatment with 1 μM GA_{12} (**1**), a common substrate for CYP714A1 and CYP714A2, promoted 74.3% germination. In contrast, treatment with 16-carboxy GA_{12} (**4**), which is a product of CYP714A1, and 12α-hydroxy GA_{12} (**13**) and GA_{53} (**14**), which are products of CYP714A2, hardly restored the non-germination phenotype of the *ga1-3* mutant. Similarly, steviol (**10**) exhibited weaker germination-inducing activity than did *ent*-kaurenoic acid (**7**) (**Table 3**). We also tested the bioactivity of 16-carboxy GA_{12} (**4**) and 12α-hydroxy GA_{12} (**13**) on the effect of rosette growth of the *ga1-3* mutant, and found that these GA compounds hardly restore growth, unlike GA_{12} (**Supplementary Table S3**). These results suggest that CYP714A1 and CYP714A2 have the potential to play a role in reducing GA activity in *Arabidopsis*.

Overexpression of *CYP714A1* causes extreme dwarfism, whereas that of *CYP714A2* causes semi-dwarfism in *Arabidopsis*

The results from biological activity studies described above indicated that *CYP714A1* and *CYP714A2* potentially encode distinct GA inactivation enzymes. To further understand the role of these enzymes, we generated transgenic *Arabidopsis* plants that overexpressed *CYP714A1* or *CYP714A2* under the control of the *Cauliflower mosaic virus* (*CaMV*) *35S* promoter. We found that the majority of *CYP714A1*-atOE lines exhibited extreme dwarfism that resembled that of *ga1-3*, while *CYP714A2*-atOE plants showed semi-dwarfism (**Fig. 4A, B**). Their dwarfism was restored by exogenously applied GA_4 (**Fig. 4C**). Both *CYP714A1*-atOE and *CYP714A2*-atOE showed a late-flowering phenotype, as seen in known GA biosynthesis mutants, including *ga1-3*, under constant light (**Fig. 4B**). The *CYP714A2*-atOE plants retained their fertility under the normal growth condition, whilst the *CYP714A1*-atOE plants needed exogenous application of GA_4 to restore their fertility (data not shown). We analyzed transcripts of *CYP714A1*-atOE and *CYP714A2*-atOE, and confirmed high accumulation [over 1000-fold compared with wild type (WT) of each transcript of the transgene] (**Supplementary Fig. S2**). Expression of the GA biosynthesis genes *GA20ox1* (*GA 20-oxidase1*) and *GA3ox1* (*GA 3-oxidase1*), both of which are negatively regulated by GA

Table 3 Biological activities of GAs on the germination of *Arabidopsis ga1-3* mutant

Compound	Concentration	Germination (%)
Mock		0 ± 0.0
GA_{12}	10 nM	1.3 ± 1.3
	100 nM	15.0 ± 1.5
	1 μM	74.3 ± 2.2
16-carboxy GA_{12}	10 nM	0 ± 0.0
	100 nM	0 ± 0.0
	1 μM	0.3 ± 0.3
12α-hydroxy GA_{12} (GA_{111})	10 nM	0 ± 0.0
	100 nM	0.7 ± 0.7
	1 μM	0 ± 0.0
13-hydroxy GA_{12} (GA_{53})	10 nM	0 ± 0.0
	100 nM	0 ± 0.0
	1 μM	0.7 ± 0.7
GA_4	10 nM	16.7 ± 0.7
	100 nM	72.3 ± 3.0
	1 μM	100 ± 0.0
GA_1	10 nM	0 ± 0.0
	100 nM	1.7 ± 0.3
	1 μM	32.0 ± 2.5
ent-Kaurenoic acid	100 nM	0.7 ± 0.7
	1 μM	2.7 ± 2.2
	10 μM	16.3 ± 4.1
Steviol (*ent*-13-hydroxy kaurenoic acid)	100 nM	0 ± 0.0
	1 μM	0 ± 0.0
	10 μM	3.3 ± 3.3

Data are mean ± SEM of triplicate tests
Mock, treatment without GA.

activity (Xu et al. 1995,Cowling et al. 1998), was highly induced in both overexpressor plants (**Supplementary Fig. S2**).

CYP714A1-overexpressor plants show severe GA deficiency and reduced sensitivity to GA_4

We further examined the *CYP714A1*-overexpressor plants that showed an extreme dwarf phenotype. GA analysis of *CYP714A1*-atOE plants (lines a4 and c2) showed that bioactive GA_4 was under the detection level limit (**Fig. 5A**, **Supplementary Table S4**). In addition, the levels of GA intermediates such as GA_{12} (**1**), GA_{15}, GA_{24} and GA_{53} (**14**) were significantly reduced in the overexpressor plants. The GA_{12} metabolite 16-carboxy GA_{12} (**4**) accumulated in the *CYP714A1*-atOE plants, but accumulated comparably in WT plants (**Fig. 5A**). In our yeast expression assay described above, GA_{12} (**1**) and GA_9 (**2**) were found to be substrates for the recombinant CYP714A1 protein, but GA_4 was not. This was unlike rice CYP714D1/EUI, which used non-13-hydroxy GAs including GA_4, but not 13-hydroxy GA including GA_1, as substrates (Zhu et al. 2006). To determine whether the bioactive GA_4 could be a substrate for CYP714A1 in planta, we examined the effect of three bioactive GAs, GA_1, GA_4 and 16,17-dihydro GA_4 (racemic mixture), on the growth of *CYP714A1*-atOE plants (lines a4 and c2). We expected that 16,17-dihydro GA_4 would not be inactivated by CYP714A1 and CYP714D1 because

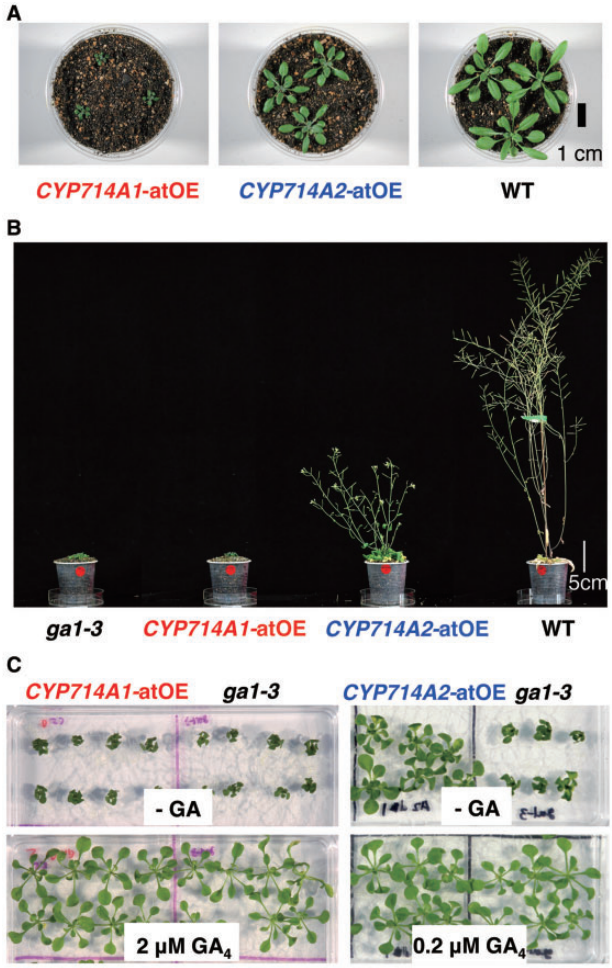

Fig. 4 *Arabidopsis* plants that overexpress the *CYP714A1* or *CYP714A2* gene. (A) Phenotype of *CYP714A1*-atOE and *CYP714A2*-atOE plants (24 days old). Bar = 1 cm. (B) Phenotype of *ga1-3*, *CYP714A1*-atOE and *CYP714A2*-atOE plants (54 days old). Bar = 5 cm. (C) Restoration of growth of *CYP714A1*-atOE and *CYP714A2*-atOE plants by exogenous application of GA_4. Sixteen-day-old seedlings of *ga1-3*, *CYP714A1*-atOE and *CYP714A2*-atOE plants are shown. They were first grown on 1/2 MS agar media for 6 d and then transferred to and grown on 1/2 MS agar media without or with GA_4 (2 or 0.2 μM).

of its structural protection at C-16 and C-17. The rosette growth of *CYP714A1*-atOE plants was comparable to that of *ga1-3* mutant plants in the absence of exogenous GA (**Fig. 5B**). The effect of the tested compounds on the growth of WT plants can be summarized as follows: GA_4 > 16,17-dihydro GA_4 > GA_1. Dose–response curves of *CYP714A1*-atOE and *ga1-3* were nearly overlapping when the plants were treated with GA_1 or 16,17-dihydro GA_4 (**Fig. 5B**). However, the dose–response curves were clearly different between *CYP714A1*-atOE and *ga1-3* when GA_4 was used; *CYP714A1*-atOE plants were less responsive to GA_4 than *ga1-3* (**Fig. 5B**). One possible explanation for these results is that GA_4, but not GA_1 and 16,17-dihydro GA_4, might be a substrate for CYP714A1 *in planta*.

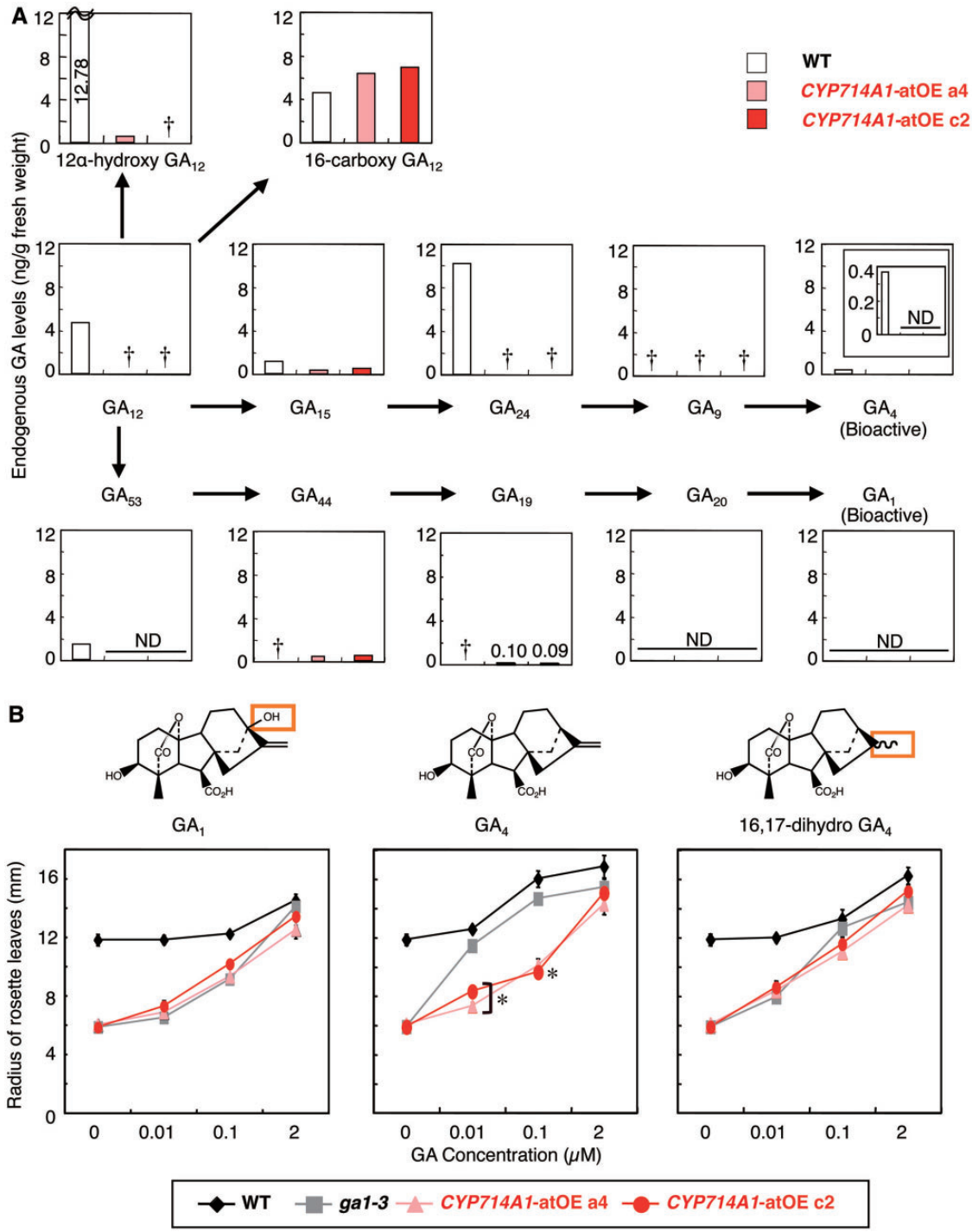

Fig. 5 Analyses of *CYP714A1*-overexpressing plants. (A) Endogenous GA levels in the aerial part of *CYP714A1*-atOE plants. GAs are shown according to the order in the biosynthesis pathway (**Fig. 1**). Results for GA_4 are also indicated in the inset with a different *y* axis scale to clarify the differences among the plants. GA analyses were repeated twice with similar results (**Supplementary Table S4**). Representative data (1st) are shown. ND, not detected; †, could not be quantified due to trace level. (B) GA_4, but not GA_1 and 16,17-dihydro GA_4, is a likely substrate for CYP714A1. Six-day-old seedlings grown on 1/2 MS agar media were transferred to 1/2 MS agar media containing various concentrations of GAs. Rosette radii of 16-day-old seedlings were measured ($n = 13–16$). Error bars represent SEM. *Significant difference between *ga1-3* and *CYP714*-atOEs (Student's *t*-test with Bonferroni correction, $P < 0.001$).

CYP714A2-overexpressor plants accumulate steviol and 13-hydroxy GAs

GA analysis of *CYP714A2*-atOE plants (lines b2 and d1) showed that the levels of non-13-hydroxy GAs [GA_{12} (**1**) GA_{15}, GA_{24} and GA_4] were decreased in these semi-dwarf plants (**Fig. 6**, **Supplementary Table S5**). In contrast, 13-hydroxy GAs (GA_{44}, GA_{19}, GA_{20} and GA_1) except GA_{53} (**14**), were highly accumulated in these plants. Our functional analysis indicates that CYP714A2 is a bifunctional enzyme that preferentially catalyzes C-13 hydroxylation of the *ent*-kaurane carbon skeleton and C-12 hydroxylation of the *ent*-gibberellane carbon skeleton (**Fig. 3**). We found that the level of *ent*-kaurenoic acid (**7**) was significantly decreased in *CYP714A2*-atOE plants; instead, steviol **(10)** accumulated to an extent more than 15-fold greater than in WT plants (**Fig. 6**). The level of 12α-hydroxy GA_{12} (**13**), another metabolite of CYP714A2 from GA_{12} (**1**), was rather low in *CYP714A2*-atOE plants. This is possibly due to the depletion of GA_{12} (**1**) precursors by 13-hydroxylation activity of CYP714A2 in the earlier steps of the GA biosynthesis pathway. Given that the bioactivity of GA_1 is much lower than that of GA_4 in plants (Talon et al. 1990, Yang et al. 1995, Cowling et al. 1998; also shown in **Fig. 5B**), our results indicate that the semi-dwarfism of *CYP714A2*-atOE plants is caused by depletion of GA_4.

Expression patterns of *CYP714A1* and *CYP714A2*

We next examined the expression profiles of the *CYP714A1* and *CYP714A2* genes in WT *Arabidopsis*. Quantitative RT-PCR analysis showed that both genes are mainly expressed in siliques, and substantially expressed in roots (**Supplementary Fig. S3A**). These expression profiles are consistent with the developmental data set of AtGenExpress, which shows that both these genes are predominantly expressed in developing seeds and siliques (**Supplementary Fig. S3B**, **C**) (Schmid et al. 2005).

Phenotype and endogenous GA levels of *cyp714a1* and *cyp714a2* mutants

To understand the physiological roles of *CYP714A1* and *CYP714A2*, we examined their T-DNA insertion mutants. *CYP714A1* and *CYP714A2* are located tandemly on chromosome 5 (**Fig. 7A**). We obtained one *cyp714a1* allele, *cyp714a1-1* (SAIL_721E01) and two *cyp714a2* alleles, *cyp714a2-1/ela2* (SALK_137272) and *cyp714a2-2* (WISC_367A10), from the *Arabidopsis* Biological Resource Center (Columbus, OH, USA) (**Fig. 7B**). Transcripts of the disrupted genes were clearly decreased compared with WT in each mutant (**Supplementary Fig. S4**). Because T-DNAs of *cyp714a1-1* and *cyp714a2-2* are located in their respective first introns, it is conceivable that each transcript detected contains intact mRNA. Even so, the

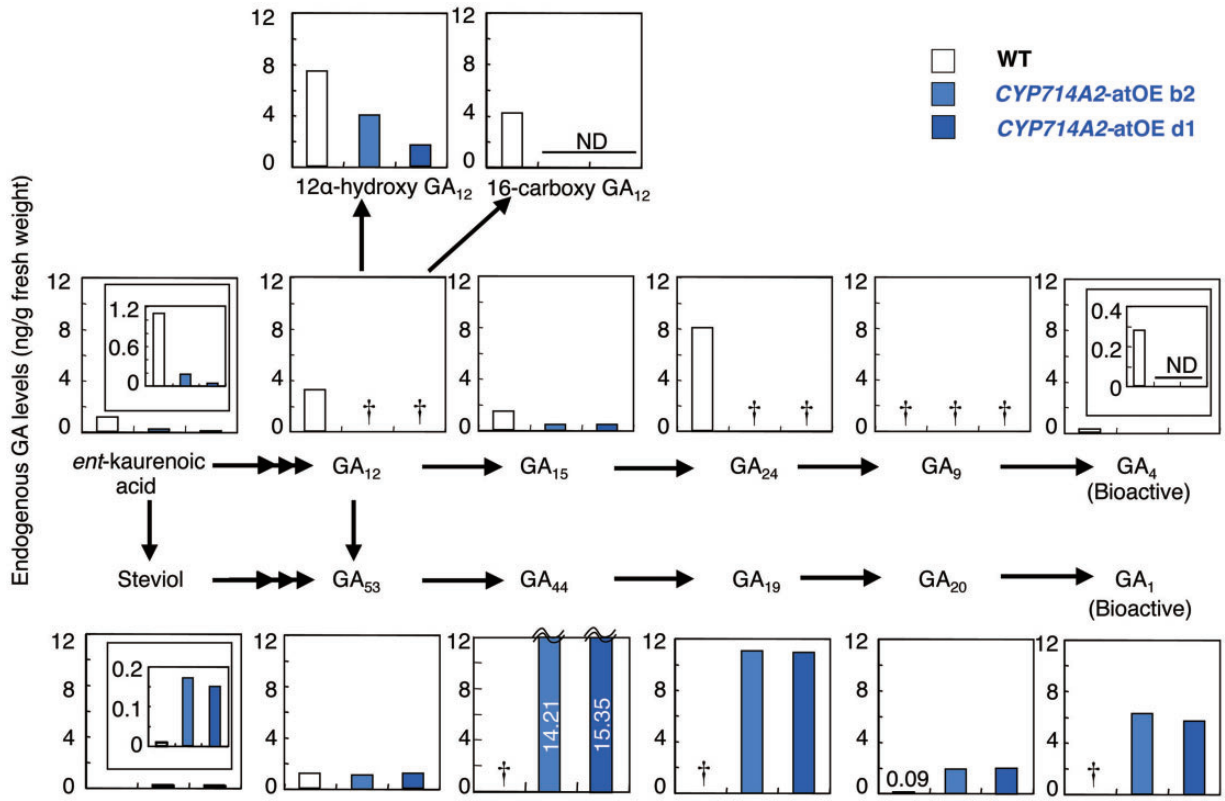

Fig. 6 Endogenous GA levels in the aerial part of *CYP714A2*-overexpressing plants. GAs are shown according to the order in the biosynthesis pathway (**Fig. 1**). Results for GA_4, *ent*-kaurenoic acid (**7**), steviol (*ent*-13-hydroxy kaurenoic acid, **10**) are also indicated in the inset with a different *y* axis scale to clarify the differences among the plants. GA analyses were repeated twice with similar results (**Supplementary Table S5**). Representative data (1st) are shown. ND, not detected; †, could not be quantified due to trace level.

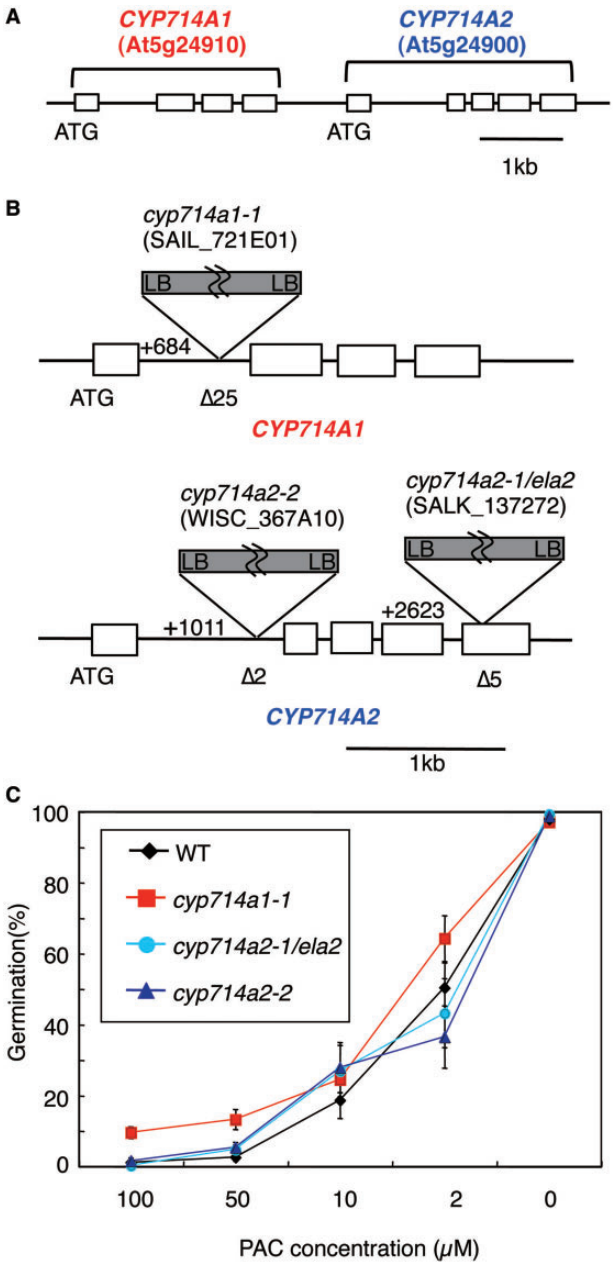

Fig. 7 Characterization of *cyp714a1* and *cyp714a2* mutants. (A) Tandem location of *CYP714A1* and *CYP714A2* genes on chromosome 5. (B) Physical map of the T-DNA insertion of the *cyp714a1* and *cyp714a2* mutants. The number denotes the distance from the initiation codon. Delta numbers denote the number of deleted nucleotides in the mutants. (C) Paclobutrazol (PAC) resistance during seed germination. Seeds were placed on filter papers soaked with water containing the indicated concentrations of PAC. Seeds were scored as germinated when radicle protrusion was visible. Values are the means ± SEM of seven or eight independent experiments.

level of each intact mRNA in these mutants was estimated at best as less than one-tenth of the WT level in *cyp714a1-1*, and at best as less than one-thousandth of the WT level in *cyp714a2-2* (**Supplementary Fig. S4**). We measured the endogenous GA levels in siliques and found that 16-carboxy GA_{12} (**4**) was significantly decreased in *cyp714a1-1* (**Supplementary Table S6**). However, the levels of other GAs, including bioactive GA_4 and GA_1 of *cyp714a1-1*, were comparable to those of WT. GA analysis of the *cyp714a2-1* and *cyp714a2-2/ela2* mutants showed that 12α-hydroxy GA_{12} (**13**) was decreased in the late stage of siliques of both mutants (**Supplementary Table S7**). However, other than this change, there is no clear difference in the gross GA profiles in both lines of mutants compared with WT (**Supplementary Table S7**). Consistent with the GA profiles, these *cyp714a1* and *cyp714a2* mutants are morphologically similar to WT under the normal growth condition (data not shown). Flowering times of these mutants were almost the same as those of WT plants under long- and short-day conditions (**Supplementary Fig. S5**). As described above, both these genes are highly expressed in developing seeds and siliques (**Supplementary Fig. S3**). We examined the seed phenotype and found that the *cyp714a1-1* mutant showed weak resistance to the GA biosynthesis inhibitor paclobutrazol (PAC) during seed germination (**Fig. 7C**). Only 2.6 and 1.0% of WT seeds germinated in the presence of 50 and 100 μM PAC, respectively, while 13.2 and 9.6% of *cyp714a1-1* seeds germinated under similar conditions.

Discussion

Previously we found that the *CYP714D1/EUI* gene encodes GA 16α,17-epoxidase, and Magome et al. (2013) reported that the *CYP714B1* and *CYP714B2* genes encode GA13ox in rice. Here, our functional analysis demonstrated that *Arabidopsis CYP714A1* and *CYP714A2* also encode distinct GA modification enzymes that oxidize various sites of C and D rings of GA compounds. Our study indicates that the metabolism of GA carried out by CYP714 family proteins is common to monocots and eudicots.

Functional analysis of the recombinant CYP714A1 protein in yeast cells showed that CYP714A1 preferentially catalyzes the conversion of GA_{12} (**1**) to 16-carboxy GA_{12} (**4**) (**Fig. 2**). Bioactivity of this GA_{12} metabolite (**Table 3**) and the GA-deficient phenotype of the *CYP714A1*-overexpressing *Arabidopsis* plants (**Fig. 4**) indicate that the 16-carboxylation of GA_{12} (**1**) is an inactivation reaction. The severe GA deficiency of the *CYP714A1* overexpressor plants can thus be explained by the depletion of precursor GAs, including GA_{12} (**1**) (**Fig. 5A**), similar to what occurs in *CYP714D1*-overexpressing rice plants (Zhu et al. 2006). Because P450s are monooxygenases (Schuler and Werck-Reichhart 2003), 16-carboxy GA_{12} (**4**) is probably produced via a multi-step reaction from GA_{12} (**1**), and no potential intermediates have been detected in our yeast expression assay. To the best of our knowledge, the occurrence of 16-carboxy GA_{12} (**4**) has not been reported in any organisms until now. We detected relatively high levels of this GA metabolite in the aerial part of the seedlings and in siliques of WT plants (**Fig. 5A** and **Supplementary Table S6**), indicating that 16-carboxy GA_{12} (**4**)

is a major GA_{12} metabolite in *Arabidopsis*. We also found increased levels of 16-carboxy GA_{12} (**4**) in *CYP714A1*-atOE plants (**Fig. 5A** and **Supplementary Table S4**) and decreased levels of this metabolite in the *cyp714a1-1* mutant (**Supplementary Table S6**). These results support the idea that CYP714A1 catalyzes the conversion of GA_{12} (**1**) to 16-carboxy GA_{12} (**4**) *in planta*. Besides 16-carboxy GA_{12} (**4**), three minor metabolites (B, C and D) were detected in our yeast expression assay (**Table 1**). Among them, metabolite B (16,17-dihydroxy-16α,17-dihydro GA_{12}, **5**), which is most likely a non-enzymatically hydrated form of 16α,17-epoxy GA_{12}, is a GA_{12} metabolite produced by the CYP714D1 protein (Zhu et al. 2006). This suggests that CYP714A1 also possesses GA 16α,17-epoxidase activity, and that the modes of catalysis of CYP714A1 and CYP714D1 therefore are in part similar to each other.

The substrate preference of CYP714A1 protein is currently unclear. The recombinant CYP714A1 was able to catalyze oxidation of GA_9 (**2**; data not shown) as well as GA_{12} (**1**), indicating that CYP714A1 is capable of catalyzing oxidation of multiple GA substrates. Our previous *in vitro* results obtained with the recombinant CYP714D1 protein indicated that 13-hydroxylation negatively affects the substrate preference of this enzyme: CYP714D1 catalyzed oxidation of non-13-hydroxy GAs (GA_{12}, GA_9 and GA_4) but not 13-hydroxy GAs (GA_{53}, GA_{20} and GA_1) (Zhu et al. 2006). The recombinant CYP714A1 protein, unlike CYP714D1 protein, did not catalyze oxidation of 13-hydroxy GAs, but also did not catalyze oxidation of a non-13-hydroxy GA, GA_4, in yeast cells (data not shown). However, *CYP714A1*-atOE plants were less sensitive to the applied GA_4 than was the *ga1-3* mutant, a difference that was not observed for GA_1 or 16,17-dihydro GA_4 (**Fig. 5B**). This observation could be explained by inactivation of GA_4 by CYP714A1 *in planta*. One possible explanation for this discrepancy is that the uptake of GA_4 by yeast cells from liquid media might not have been efficient for some unknown reason. To eliminate this possibility, *in vitro* functional analysis of CYP714A1 using a microsome fraction would be needed.

In contrast to the severe dwarf phenotype of the CYP714A1 overexpressor plants (**Fig. 4A, B**), the loss of function mutant *cyp714a1-1* shows a subtle GA-related phenotype in the presence of a GA biosynthesis inhibitor (**Fig. 7C**). In addition, our GA analysis of siliques of this mutant showed that there was no significant change in bioactive GA levels (GA_4 and GA_1) compared with those in WT, while the levels of 16-carboxy GA_{12} (**4**) were significantly decreased (27% of the WT level) (**Supplementary Table S6**). It has been reported that another *cyp714a1/ela1* mutant (SALK_016089) also had no visible phenotype (Zhang et al. 2011). One possible reason for the small impact of the disruption of this gene on bioactive GA levels is the presence of other GA inactivation enzymes in the siliques. Five C_{19}-*GA2ox* genes (*GA2ox1*, *-2*, *-3*, *-4* and *-6*), encoding 2ODD enzymes, are expressed in *Arabidopsis* siliques (Rieu et al. 2008). Reduced fertility, possibly due to the unequal elongation of pistils and stamens, was observed in the *ga2ox quintuple* mutant but not in each single mutant (Rieu et al. 2008). Furthermore, the GA methyltransferase genes (*GAMT1* and *GAMT2*) are also highly expressed in the siliques (Varbanova et al. 2007). To clarify the physiological role of the *CYP714A1* gene in siliques, preparation of multiple mutants with defects in other GA inactivation enzyme genes might be required.

Our functional analysis of the recombinant CYP714A2 protein showed that this P450 enzyme possesses 12α-hydroxylation and/or 13-hydroxylation activities using early GA intermediates in the GA biosynthesis pathway (*ent*-kaurenoic acid, **7**; *ent*-7α-hydroxy kaurenoic acid, **8**; GA_{12}-7-aldehyde, **9**; and GA_{12}, **1**) as substrates (**Fig. 1**). In particular, *ent*-kaurenoic acid (**7**) and *ent*-7α-hydroxy kaurenoic acid (**8**) were predominantly metabolized into steviol (*ent*-13-hydroxy kaurenoic acid, **10**) and probably to *ent*-7α,13-dihydroxy kaurenoic acid (**11**), respectively (**Fig. 3B**, **Table 2**, **Supplementary Table S2**). These results suggest that CYP714A2 may contribute to producing 13-hydroxy GAs in *Arabidopsis*, even though GA_{12} is not its substrate (as has been predicted), but, rather, more upstream precursors (**Fig. 1**). The following results and facts support our speculation. First, steviol (**10**) exists in WT *Arabidopsis* plants (**Fig. 6**, **Supplementary Table S5**). Second, steviol (**10**) and almost all 13-hydroxy GAs accumulated in *Arabidopsis* plants that overexpressed *CYP714A2* (**Fig. 6**, **Supplementary Table S5**). Third, *CYP714A2* is predominantly expressed in developing seeds and siliques (**Supplementary Fig. S3**), in which 13-hydroxy GAs, including GA_1, are highly accumulated in *Arabidopsis* (Varbanova et al. 2007, Kanno et al. 2010). Finally, other CYP714 members, such as rice CYP714B1 and CYP714B2, encode GA13ox, although they catalyze the 13-hydroxylation of GA_{12} (**1**) but not that of *ent*-kaurenoic acid (**7**) (Magome et al. 2013). *Arabidopsis* plants that overexpress *CYP714B1* or *CYP714B2* show semi-dwarfism with increased levels of 13-hydroxy GAs, including GA_1 (Magome et al. 2013). However, our GA analysis of siliques of *cyp714a2-1* and *cyp714a2-2* showed that there is no significant change in GA 13-hydroxylation in both mutant alleles compared with WT (**Supplementary Table S7**). One possible reason for this result is the likely presence of other GA13oxs in *Arabidopsis*. Although cytochrome P450s are usually membrane-bound proteins, GA 13-hydroxylation activity was found in a soluble fraction of spinach leaves (Gilmour et al. 1986). Recombinant TaGA3ox2 protein (a GA3ox from wheat) exhibits weak GA13ox activity, in addition to GA3ox activity in vitro (Appleford et al. 2006). Recently, a P450 gene that encodes *ent*-kaurenoic acid 13-oxidase and probably belongs to the CYP72A subfamily was found in stevia (*Stevia rebaudiana*) (Brandle and Telmer 2007). These orthologs of *Arabidopsis* may play a role in the GA13-hydroxylation in siliques.

Our bioactivity tests indicate that the 12α-hydroxylation of GA_{12} (**1**) by CYP714A2 is an inactivation pathway (**Table 3**, **Supplementary Table S3**). The level of 12α-hydroxy GA_{12} (**13**) was rather decreased in the *CYP714A2* at OE plants (**Fig. 6**, **Supplementary Table S5**). This is possibly due to the

depletion of GA_{12} precursors by the 13-hydroxylation activity of CYP714A2 in earlier steps of the GA biosynthesis pathway in the transgenic plants. This result does not, therefore, necessarily mean that the 12α-hydroxylation activity of CYP714A2 is improbable *in planta*. Indeed, decreased levels of 12α-hydroxy GA_{12} (**13**) at the late stage of siliques of *cyp714a2* mutants (**Supplementary Table S7**) indicate that CYP714A2 protein plays a role in GA 12α-oxidase activity in *Arabidopsis*. In contrast, no reduction in the levels of 12α-hydroxy GA_{12} (**13**) in the early stage of siliques of the mutant (**Supplementary Table S7**) suggests the presence of other GA 12α-oxidases. The 12α-hydroxylated GA_{12} (**13**) has been found in various plants, such as the seeds of pumpkin (Blechschmidt et al. 1984) and sporophytes of the tree ferns *Cybotium glaucum* and *Dicksonia antarctica* (Yamane et al. 1988), suggesting that this pathway is common to many plant species. In addition, the 12α,13-dihydroxy GA_{12} (GA_{123}, **16**), which is one of the GA_{12} metabolites produced by CYP714A2 (**Table 2**), was also found in immature fruits of strawberry (*Fragaria* × *ananassa*) (Blake et al. 2000).

P450s share the same CYP number when their sequence identity is typically >40%; they are further grouped into subfamilies (indicated by letters) based on sequence identity >50% (Schuler and Werck-Reichhart 2003). In this study, we demonstrated that although CYP714A1 and rice CYP714D1 (38.8% identity; **Supplementary Table S1**) are classified in different subfamilies, they are functionally similar as GA inactivation enzymes (C16, C17 oxidation). Both CYP714A2 and rice CYP714Bs (41.2–42.0% identity) possess GA 13-hydroxylation activity. Furthermore, we have also demonstrated that CYP714A1 and CYP714A2 (73.1% identity) possess distinct enzyme activities, even though they are classified in the same subfamily. The diversity of CYP714 family members makes it difficult to speculate on the function of the CYP714 proteins based only on their primary structures. Recently, a similar functional diversity has been reported for the rice CYP701A/*ent*-kaurene oxidase (KO) subfamily, showing that CYP701A8 (a KO paralog) likely plays a role in the production of diterpenoid phytoalexins, but not in GA biosynthesis (Wang et al. 2012).

The current model for the contribution of CYP714A1 and CYP714A2 to GA metabolism is shown in **Fig. 8**. CYP714A1 would play a role in the inactivation of non-13-hydroxy GAs such as GA_{12} (**1**), GA_9 (**2**) and possibly GA_4 by C16-carboxylation or a similar oxidation. CYP714A2 would play a role in the C13-hydroxylation using *ent*-kaurenoic acid (**7**) and *ent*-7α-hydroxy kaurenoic acid (**8**) as substrates. This leads to the production of weakly bioactive GA_1 via the early GA 13-hydroxylation pathway. Although it is unclear whether *ent*-kaurenoic acid oxidases (KAOs) metabolize 13-hydroxy substrates, accumulation of GA_1 in the *CYP714A2* overexpressor plants (**Fig. 6**, **Supplementary Table S5**) supports our idea. Besides 13-oxidase, CYP714A2 would also act as a 12α-oxidase when GA_{12}-7-aldehyde (**9**) and GA_{12} (**1**) are its substrates. Therefore, both CYP714A1 and CYP714A2 would compete for the non-13-hydroxy substrates (**Fig. 8**). These competitive activities would determine the ratio of the strongly active GA (GA_4)

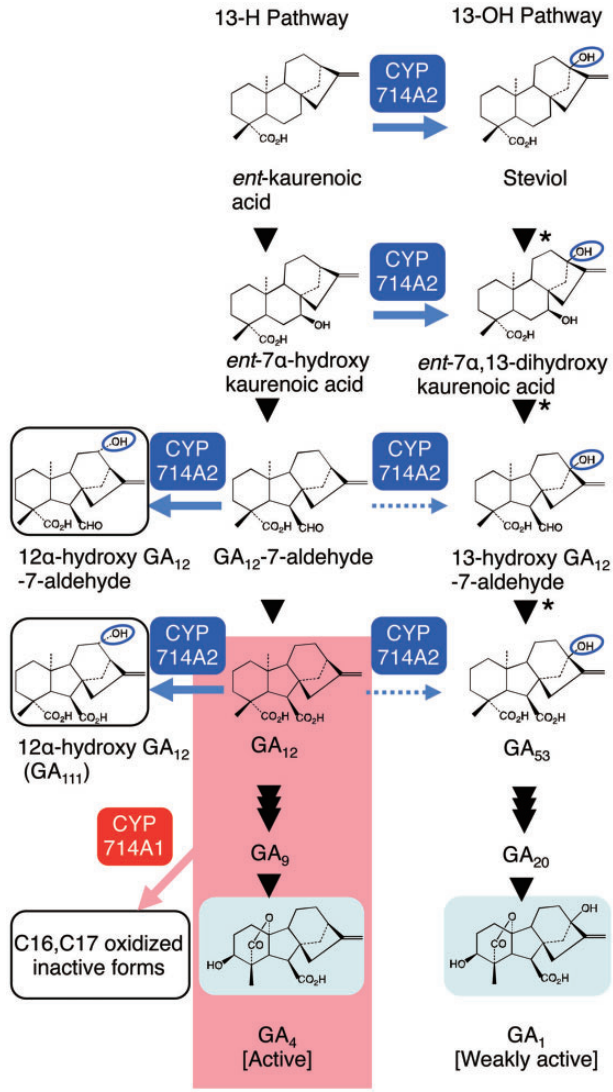

Fig. 8 Proposed model for the roles of CYP714A1 and CYP714A2 in GA metabolism. Black arrowheads indicate the flow of the GA biosynthesis pathway. The biosynthesis pathway from steviol (*ent*-13-hydroxy kaurenoic acid) to 13-hydroxy GA_{12} (GA_{53}) (indicated by *) has not been experimentally demonstrated (see text). The red square box and arrow indicate substrates of CYP714A1 and its inactivation activity. Blue arrows indicate strong (solid) or weak (dotted) 12α-hydroxylation/13-hydroxylation activities of CYP714A2.

and the weakly active one (GA_1), as is the case with the CYP714D1 and CYP714Bs in rice (Magome et al. 2013).

The physiological roles of CYP714A1 and CYP714A2 are unclear. Intriguingly, Zhang et al. (2011) reported that *CYP714A1* and *CYP714A2* double knockdown plants made by the combinational use of T-DNA insertion and RNA interference (RNAi) showed increased above-ground biomass and early flowering with increased levels of bioactive GA_4. These phenotypes might be explained as a consequence of double blocking of the CYP714A1 and CYP714A2 pathways (**Fig. 8**). However, GA_1 levels of the double knockdown plants were comparable to those of WT (Zhang et al. 2011), indicating that GA 13-

hydroxylation is not blocked in these plants. In addition, the transcript levels of *CYP714A1* and *CYP714A2* are very low in above-ground tissues, except for developing seeds and siliques in WT (**Supplementary Fig. S3**). These results seem inconsistent with the outstanding GA overdose phenotype. Further studies would be needed to reveal the cause of the double knockdown phenotype.

The steviol (**10**) synthase activity of CYP714A2 shows promise for applications other than plant growth regulation. Steviol (**10**) is an aglycone of stevioside, a natural sweetener produced by stevia (*S. rebaudiana*) (reviewed by Brandle and Telmer 2007). We found that steviol (**10**) can be accumulated by overexpressing the *CYP714A2* gene in yeast and *Arabidopsis* (**Figs 3B, 6**), demonstrating the potential for efficient stevioside production in heterologous organisms using biotechnological approaches.

Materials and Methods

Plant materials and growth conditions

Arabidopsis thaliana ecotype Columbia-0 (Col-0) was used as the WT. The T-DNA tagged mutants *cyp714a1-1* (SAIL_721E01), *cyp714a2-1/ela2* (SALK_137272) and *cyp714a2-2* (WISC_367A10) were provided by the *Arabidopsis* Biological Resource Center (Columbus, OH, USA). *ga1-3* mutant (backcrossed six times to Col-0 plants) has been described previously (Mitchum et al. 2006). Plants were grown on soil (mold:vermiculite = 1:1, v/v) or 1/2 Murashige–Skoog (MS) agar media (Murashige and Skoog 1962) under constant light conditions (approximately 60 μmol m^{-2} s^{-1}) at 22°C unless otherwise specified.

Heterologous expression in yeast and identification of CYP714As metabolites

Coding regions of *CYP714A1* and *CYP714A2* were amplified from cDNA clones using sets of primers (**Supplementary Table S8**). The PCR products were ligated into pCR2.1 vector plasmid (Life Technologies Corporation, Carlsbad, CA USA). After confirmation of the nucleotide sequence, the plasmid DNAs were digested with BamHI and KpnI, and the DNA fragment containing the cloned DNAs was ligated into pYeDP60 vector. The resulting plasmid was transformed into yeast strain WAT11 engineered to co-produce the *Arabidopsis* NADPH P450 reductase-1 (Pompon et al. 1996). Functional analyses of CYP714A1 and CYP714A2 were performed by in vivo bioconversion (Pompon et al. 1996). The transformed colonies were inoculated into 10 ml of SGI medium (Pompon et al. 1996) and were grown at 30°C for 1 d in a shaking incubator (200 rpm). One milliliter of SGI-cultured yeast medium was inoculated into 10 ml of SLI medium (Pompon et al. 1996) and grown at 28°C for 1 d until the cell density reached 4×10^7 cells ml^{-1}. The medium was diluted with fresh SLI medium to obtain 4×10^6 cells ml^{-1}. Five milliliters of the diluted medium was incubated with 1 μg of a GA substrate at 28°C for 16 h until the cell density reached 5×10^7 cells ml^{-1}. The GA products were extracted with ethyl acetate. The ethyl acetate phase was partitioned against 0.5 M K_2HPO_4 buffer (pH 9). The buffer phase was adjusted to pH 3 with 6 N HCl and extracted with ethyl acetate. The acidic ethyl acetate phase was evaporated to dryness. The residual solid was dissolved in 5% methanol (including 1% acetic acid) and loaded onto a Bond Elut C18 column (ODS, Agilent Technologies, Santa Clara, CA USA) that was eluted with 80% methanol after washing with 1% acetic acid. The metabolites of *ent*-kaurenoic acid (**7**), *ent*-7α-hydroxy kaurenoic acid (**8**) and GA_{12}-7-aldehyde (**9**) were extracted with *n*-hexane, followed by *n*-hexane-ethyl acetate (1:1) and ethyl acetate. The extracts obtained with these three kinds of solvents were combined and evaporated to dryness. The residual solid was dissolved in 90% methanol and passed through a Bond Elut C18 column. The column eluates were evaporated to dryness and derivatized with diazomethane and/or *N*-methyl-*N*-(trimethylsilyl)trifluoroacetamide. GC-MS analysis of the samples was performed as described previously (Zhu et al. 2006).

Chemical synthesis of 16-carboxy GA_{12} (16-carboxy-16β,17-dihydro GA_{12}) trimethyl ester

Following procedures reported by Gaskin et al. (1992) and Seto et al. (1995), an authentic sample was prepared from GA_{12} dimethyl ester by treatment with diborane to give a mixture of epimeric 16,17-dihydro-17-ols, which were oxidized with Dess-Martin reagent to the corresponding aldehydes. Base-catalyzed equilibration then afforded the 16α-epimer, which was oxidized with Jones reagent to 16-carboxy-16β,17-dihydro GA_{12} (**4**). Then, diazomethane treatment produced the trimethyl ester. Details will be published elsewhere.

Enzymatic preparation of 16-carboxy GA_{12} and 12α-hydroxy GA_{12}

16-Carboxy GA_{12} (**4**) and 12α-hydroxy GA_{12} (**13**) were prepared by incubation of GA_{12} (**1**; 50 μg) with the recombinant yeast cultures (50 ml), producing CYP714A1 and CYP714A2, respectively. The acidic ethyl acetate-soluble phase was purified by reversed-phase HPLC using a CAPCELL PAK C18 TYPE SG120Å column (250 × 6 mm i.d.; Shiseido Company, Ltd, Tokyo Japan) eluted with the following methanol–water (including 0.1% acetic acid) gradient at a flow rate of 1.5 ml min^{-1}: 0–5 min, 20% methanol; 5–40 min, 20–80% methanol; and 40–50 min, 80% methanol. Fractions were collected every minute. The column oven temperature was maintained at 40°C. The following fractions were collected: fraction 34/35 (for 12α-dihydroxy GA_{12}), 37/38 (for 16-carboxy GA_{12}) and 44/45 (for remaining GA_{12}). The concentrations of 16-carboxy and 12α-dihydroxy derivatives were estimated from these conversion rates, based on the assumption that their recoveries were 100%. For quantification of endogenous 16-carboxy GA_{12} (**4**) in plants, its ^{2}H-labeled internal standard ([16-^{2}H] 16-carboxy GA_{12}) was prepared by incubating [17,17-$^2H_2$] GA_{12} with the CYP714A1-producing yeast culture (see Results).

Bioassay of GA metabolites

The *ga1-3* mutant was used to test the biological activities of GAs. In the seed germination assay, *ga1-3* seeds (about 50 seeds) that were washed with 0.02% (w/v) Tween 20 were imbibed in water with or without various GAs at 4°C for 4 d and then germinated on a filter paper (3MM; GE Healthcare UK Ltd, Little Chalfont, UK) soaked with water with or without various GAs at 22°C under continuous light (36 μmol m^{-2} s^{-1}) for 3 d. Seeds were scored as germinated when radicle protrusion was visible. To evaluate rosette growth, *ga1-3* seeds were stratified in the presence of 50 μM GA_4 in the dark at 4°C for 4 d. The seeds were washed with sterile water five times to remove excess GA_4, placed on 1/2 MS agar medium and then incubated for 9 d. The grown seedlings were transplanted onto new 1/2 MS agar media with or without GAs. After 6 d, the diameters of the rosettes were measured ($n = 5$). The assays were performed using triplicate samples.

Transgenic plant construction

To construct transgenic plants overexpressing *CYP714A1* or *CYP714A2* (*CYP714A1*- or *CYP714A2*-atOE), coding regions of *CYP714A1* and *CYP714A2* were amplified from cDNA clones using sets of primers (**Supplementary Table S8**). The PCR products were ligated into pCR2.1 vector plasmid (Life Technologies Corporation, Carlsbad, CA USA). After confirmation of the nucleotide sequence, the plasmid DNAs were digested with BamHI and PstI, and a DNA fragment containing the cloned DNA was inserted between the CaMV 35S promoter and the nopaline synthase terminator of the pCGN vector. *Agrobacterium* (strain EHA105)-mediated transformation of WT was conducted as described (Magome et al. 2004). Homozygous T3 plants were used for analysis.

Quantification of GAs

For quantitative GA analysis of *CYP714A1* or *CYP714A2*-atOE plants, aerial parts of the overexpressor plants grown on soil were harvested just before bolting and were stored at −80°C. To analyze siliques of *cyp714a1*, late-stage siliques (stages 5–10) were collected. For analysis of *cyp714a2* mutants, early-stage siliques (stages 3–5) as well as the late-stage siliques were collected. Stages of siliques were defined according to Bowman (1994) and Kleindt et al. (2010). The GA content was determined by liquid chromatography-selected reaction monitoring as previously described (Varbanova et al., 2007).

GA and paclobutrazol treatments

For the GA treatment of *CYP714A1*-atOE plants (**Fig. 5B**), 6-day-old seedlings grown on 1/2 MS agar plates were transferred onto 1/2 MS agar plates containing various concentrations (0, 0.01, 0.1 or 2 μM) of each GA compound. Rosette radii of 16-day-old seedlings were measured ($n = 13–16$). To study the effect of PAC treatment on seed germination (**Fig. 7C**), the seeds were stored at room temperature at 30% humidity for at least 2 months to allow after-ripening. Seeds (60–100) were incubated on wet filter paper (3MM; GE Healthcare UK Ltd. Little Chalfont, UK) containing various concentrations (0, 2, 10, 50 or 100 μM) of PAC. Seeds were scored as germinated when radicle protrusion was visible.

Real time quantitative RT-PCR

Total RNA of siliques was isolated using the RNAqueous RNA Isolation Kit with Plant RNA Isolation Aid (Life Technologies Corporation, Carlsbad, CA USA). Total RNA of other tissues was isolated using the RNeasy extraction kit (Qiagen, Hilden, Germany). Real-time quantitative RT-PCR using an ABI Prism 7700 sequence detection system (Life Technologies Corporation) was described previously (Magome et al., 2004). 18S rRNA was used for normalization. Specific primers and probes used in this study are listed in **Supplementary Table S8**.

Supplementary data

Supplementary data are available at PCP online.

Funding

This work was supported by RIKEN Plant Science Center.

Acknowledgements

We thank Ms Akiko Onozuka and Ms Yoko Sato for dedicated technical assistance.

Conflicts of interest

No conflicts of interest declared.

References

Appleford, N.E., Evans, D.J., Lenton, J.R., Gaskin, P., Croker, S.J., Devos, K.M. et al. (2006) Function and transcript analysis of gibberellin-biosynthetic enzymes in wheat. *Planta* 223: 568–582.

Blake, P.S., Taylor, D.R., Crisp, C.M., Mander, L.N. and Owen, D.J. (2000) Identification of endogenous gibberellins in strawberry, including the novel gibberellins GA_{123}, GA_{124} and GA_{125}. *Phytochemistry* 55: 887–890.

Blechschmidt, S., Castel, U., Gaskin, P., Hedden, P., Graebe, J.E. and Macmillan, J. (1984) GC/MS analysis of the plant hormones in seeds of *Cucurbita maxima*. *Phytochemistry* 23: 553–558.

Bowman, J.L. (1994) *Arabidopsis*: an Atlas of Morphology and Development. Springer-Verlag, New York.

Brandle, J.E. and Telmer, P.G. (2007) Steviol glycoside biosynthesis. *Phytochemistry* 68: 1855–1863.

Busov, V.B., Meilan, R., Pearce, D.W., Ma, C., Rood, S.B. and Strauss, S.H. (2003) Activation tagging of a dominant gibberellin catabolism gene (GA 2-oxidase) from poplar that regulates tree stature. *Plant Physiol.* 132: 1283–1291.

Cowling, R.J., Kamiya, Y., Seto, H. and Harberd, N.P. (1998) Gibberellin dose-response regulation of *GA4* gene transcript levels in *Arabidopsis*. *Plant Physiol.* 117: 1195–1203.

Fleet, C.M. and Sun, T.P. (2005) A DELLAcate balance: the role of gibberellin in plant morphogenesis. *Curr. Opin. Plant Biol.* 8: 77–85.

Gaskin, P., Hoad, G.V., Macmillan, J., Makinson, I.K. and Readman, J.E. (1992) Gibberellins A_{82} and A_{83} in seed of *Lupinus albus*. *Phytochemistry* 31: 1869–1877.

Gaskin, P. and Macmillan, J. (1991) *GC-MS of the Gibberellins and Related Compounds: Methodlogy and a Library of Spectra*. University of Bristol Cantock's Enterprises, Bristol, UK.

Gilmour, S.J., Zeevaart, J.A.D., Schwenen, L. and Graebe, J.E. (1986) Gibberellin metabolism in cell-free-extracts from spinach leaves in relation to photoperiod. *Plant Physiol.* 82: 190–195.

Helliwell, C.A., Poole, A., Peacock, W.J. and Dennis, E.S. (1999) *Arabidopsis ent*-kaurene oxidase catalyzes three steps of gibberellin biosynthesis. *Plant Physiol.* 119: 507–510.

Kanno, Y., Jikumaru, Y., Hanada, A., Nambara, E., Abrams, S.R., Kamiya, Y. et al. (2010) Comprehensive hormone profiling in developing *Arabidopsis* seeds: examination of the site of ABA biosynthesis, ABA transport and hormone interactions. *Plant Cell Physiol.* 51: 1988–2001.

Kleindt, C.K., Stracke, R., Mehrtens, F. and Weisshaar, B. (2010) Expression analysis of flavonoid biosynthesis genes during *Arabidopsis thaliana* silique and seed development with a primary focus on the proanthocyanidin biosynthetic pathway. *BMC Res Notes* 3: 255.

Lester, D.R., Ross, J.J., Smith, J.J., Elliott, R.C. and Reid, J.B. (1999) Gibberellin 2-oxidation and the *SLN* gene of *Pisum sativum*. *Plant J.* 19: 65–73.

Luo, A.D., Qian, Q., Yin, H.F., Liu, X.Q., Yin, C.X., Lan, Y. et al. (2006) *EUI1*, encoding a putative cytochrome P450 monooxygenase, regulates internode elongation by modulating gibberellin responses in rice. *Plant Cell Physiol.* 47: 181–191.

Magome, H., Nomura, T., Hanada, A., Takeda-Kamiya, N., Ohnishi, T., Shinma, Y. et al. (2013) *CYP714B1* and *CYP714B2* encode gibberellin 13-oxidases that reduce gibberellin activity in rice. *Proc. Natl Acad. Sci. U. S. A.* 110: 1947–1952.

Magome, H., Yamaguchi, S., Hanada, A., Kamiya, Y. and Oda, K. (2004) *dwarf and delayed-flowering 1*, a novel *Arabidopsis* mutant deficient in gibberellin biosynthesis because of overexpression of a putative AP2 transcription factor. *Plant J.* 37: 720–729.

Mansuy, D., Leclaire, J., Fontecave, M. and Momenteau, M. (1984) Oxidation of monosubstituted olefins by cytochromes P-450 and heme models: evidence for the formation of aldehydes in addition to epoxides and allylic alcohols. *Biochem. Biophys. Res. Commun.* 119: 319–325.

Martin, D.N., Proebsting, W.M. and Hedden, P. (1999) The *SLENDER* gene of pea encodes a gibberellin 2-oxidase. *Plant Physiol.* 121: 775–781.

Mitchum, M.G., Yamaguchi, S., Hanada, A., Kuwahara, A., Yoshioka, Y., Kato, T. et al. (2006) Distinct and overlapping roles of two gibberellin 3-oxidases in *Arabidopsis* development. *Plant J.* 45: 804–818.

Murashige, T. and Skoog, F. (1962) A revised medium for rapid growth and bio assays with tobacco tissue cultures. *Physiol. Plant.* 15: 473–497.

Nakajima, M., Shimada, A., Takashi, Y., Kim, Y.C., Park, S.H., Ueguchi-Tanaka, M. et al. (2006) Identification and characterization of *Arabidopsis* gibberellin receptors. *Plant J.* 46: 880–889.

Nomura, T., Kushiro, T., Yokota, T., Kamiya, Y., Bishop, G.J. and Yamaguchi, S. (2005) The last reaction producing brassinolide is catalyzed by cytochrome P-450s, CYP85A3 in tomato and CYP85A2 in *Arabidopsis*. *J. Biol Chem* 280: 17873–17879.

Pompon, D., Louerat, B., Bronine, A. and Urban, P. (1996) Yeast expression of animal and plant P450s in optimized redox environments. *Methods Enzymol.* 272: 51–64.

Rieu, I., Eriksson, S., Powers, S.J., Gong, F., Griffiths, J., Woolley, L. et al. (2008) Genetic analysis reveals that C_{19}-GA 2-oxidation is a major gibberellin inactivation pathway in *Arabidopsis*. *Plant Cell* 20: 2420–2436.

Sakamoto, T., Kobayashi, M., Itoh, H., Tagiri, A., Kayano, T., Tanaka, H. et al. (2001) Expression of a gibberellin 2-oxidase gene around the shoot apex is related to phase transition in rice. *Plant Physiol.* 125: 1508–1516.

Schmid, M., Davison, T.S., Henz, S.R., Pape, U.J., Demar, M., Vingron, M. et al. (2005) A gene expression map of *Arabidopsis thaliana* development. *Nat. Genet.* 37: 501–506.

Schneider, G. and Schliemann, W. (1994) Gibberellin conjugates - an overview. *Plant Growth Regul.* 15: 247–260.

Schomburg, F.M., Bizzell, C.M., Lee, D.J., Zeevaart, J.A. and Amasino, R.M. (2003) Overexpression of a novel class of gibberellin 2-oxidases decreases gibberellin levels and creates dwarf plants. *Plant Cell* 15: 151–163.

Schuler, M.A. and Werck-Reichhart, D. (2003) Functional genomics of P450s. *Annu. Rev. Plant Biol.* 54: 629–667.

Seto, H., Sassa, T., Kawaide, H., Shigihara, T., Uzawa, J. and Yoshida, S. (1995) Isolation and stereocontrolled synthesis of a 17-hydroxy-16β,17-dihydrogibberellin, GA_{82}. *Tetrahedron Lett.* 36: 5917–5920.

Sun, T.P. and Kamiya, Y. (1994) The *Arabidopsis GA1* locus encodes the cyclase *ent*-kaurene synthetase A of gibberellin biosynthesis. *Plant Cell* 6: 1509–1518.

Talon, M., Koornneef, M. and Zeevaart, J.A. (1990) Endogenous gibberellins in *Arabidopsis thaliana* and possible steps blocked in the biosynthetic pathways of the semidwarf *ga4* and *ga5* mutants. *Proc. Natl Acad. Sci. U. S. A.* 87: 7983–7987.

Thomas, S.G., Phillips, A.L. and Hedden, P. (1999) Molecular cloning and functional expression of gibberellin 2- oxidases, multifunctional enzymes involved in gibberellin deactivation. *Proc. Natl Acad. Sci. U. S. A.* 96: 4698–4703.

Ueguchi-Tanaka, M., Ashikari, M., Nakajima, M., Itoh, H., Katoh, E., Kobayashi, M. et al. (2005) *GIBBERELLIN INSENSITIVE DWARF1* encodes a soluble receptor for gibberellin. *Nature* 437: 693–698.

Ueguchi-Tanaka, M., Nakajima, M., Katoh, E., Ohmiya, H., Asano, K., Saji, S. et al. (2007) Molecular interactions of a soluble gibberellin receptor, GID1, with a rice DELLA protein, SLR1, and gibberellin. *Plant Cell* 19: 2140–2155.

Varbanova, M., Yamaguchi, S., Yang, Y., McKelvey, K., Hanada, A., Borochov, R. et al. (2007) Methylation of gibberellins by *Arabidopsis* GAMT1 and GAMT2. *Plant Cell* 19: 32–45.

Wang, Q., Hillwig, M.L., Wu, Y.S. and Peters, R.J. (2012) CYP701A8: a rice *ent*-kaurene oxidase paralog diverted to more specialized diterpenoid metabolism. *Plant Physiol.* 158: 1418–1425.

Xu, Y.L., Li, L., Wu, K., Peeters, A.J., Gage, D.A. and Zeevaart, J.A. (1995) The *GA5* locus of *Arabidopsis thaliana* encodes a multifunctional gibberellin 20-oxidase: molecular cloning and functional expression. *Proc. Natl Acad. Sci. U. S. A.* 92: 6640–6644.

Yamaguchi, S. (2008) Gibberellin metabolism and its regulation. *Annu. Rev. Plant Biol.* 59: 225–251.

Yamane, H., Fujioka, S., Spray, C.R., Phinney, B.O., Macmillan, J., Gaskin, P. et al. (1988) Endogenous gibberellins from sporophytes

of two tree ferns, *Cibotium glaucum* and *Dicksonia antarctica*. *Plant Physiol.* 86: 857–862.

Yang, Y.Y., Nagatani, A., Zhao, Y.J., Kang, B.J., Kendrick, R.E. and Kamiya, Y. (1995) Effects of gibberellins on seed germination of phytochrome-deficient mutants of *Arabidopsis thaliana*. *Plant Cell Physiol.* 36: 1205–1211.

Zhang, Y.Y., Zhang, B.C., Yan, D.W., Dong, W.X., Yang, W.B., Li, Q. et al. (2011) Two *Arabidopsis* cytochrome P450 monooxygenases, CYP714A1 and CYP714A2, function redundantly in plant development through gibberellin deactivation. *Plant J.* 67: 342–353.

Zhu, Y., Nomura, T., Xu, Y., Zhang, Y., Peng, Y., Mao, B. et al. (2006) *ELONGATED UPPERMOST INTERNODE* encodes a cytochrome P450 monooxygenase that epoxidizes gibberellins in a novel deactivation reaction in rice. *Plant Cell* 18: 442–456.